Itinerant Oscillator Model

Evaluation Using Experimental Results for the Disordered Solid 1,2,3-Trichlorotrimethyl Benzene

By Gareth J. Evans* and Myron W. Evans

Edward Davies Chemical Laboratories,
University College of Wales, Aberystwyth SY23 1NE

and

W. T. Coffey

School of Engineering, Trinity College, Dublin 2

Received 22nd March, 1978

By consideration of a suitable approximation to the Liouville equation it is shown analytically that in the disordered solid state of 1,2,3-trichlorotrimethyl benzene (TCTMB) the total zero to THz loss profile consists of two peaks separated by many decades of frequency. Neither the low frequency nor THz loss peaks should be modelled independently, as has been the practice in the past. The molecular dynamics may be represented by physically interpreting the particular Mori approximant we have used. This may be achieved either in terms of the itinerant librator or in terms of dipole–dipole coupling.

It has been the practice [1, 2] recently in the literature to model separately the radio frequency and far infrared (THz) loss peaks in the disordered solid state [3] of disc-like molecules such as trichlorotrimethylbenzene (TCTMB). For instance, the broad low frequency peak has been described in terms of rotational diffusion,[1] which is well known [4] to be unacceptable at high frequencies since a plateau absorption appears in the power absorption coefficient $\alpha(\omega)$. This is caused by neglect of inertial effects and also by the absence of a dynamical mechanism by which resonance absorption [5] may be described, rising above the plateau in $\alpha(\omega)$. The far infrared absorption peak has been recognized by Darmon and Brot [2] as librational in origin, but was modelled in terms of a harmonic oscillator mechanism producing a delta function absorption at the peak of the broad band actually observable. No account was taken of the kHz loss peak. The radio frequency and THz losses are clearly manifestations of the same overall dynamical evolution and are recognized as such in the literature. Therefore in this paper we attempt to describe them as such by using a more realistic approximation of the Liouville equation than either of rotational diffusion or harmonic oscillation.

We use an approximant of the Mori continued fraction which may be interpreted physically [6] in terms of an itinerant librator with an extra friction term between the inner molecule and its cage of nearest neighbours. This is a realistic model for the TCTMB reorientations, which take place in a plane about the molecular hexad axes. The same approximant may denote physically a mechanism of dipole–dipole coupling superimposed upon the itinerant libration.[7]

THEORETICAL SYNOPSIS

The dynamical evolution is described on a molecular scale by the Liouville equation which may be written in the form:[8]

$$\dot{A}(t) = i\Omega_A A(t) - \int_0^t d\tau\, \phi_A(t-\tau)A(\tau) + F_A(t). \tag{1}$$

Here $A(t)$ is an $n \times 1$ column vector, with elements $A_j(t)$ which are linearly independent, real-valued (implicitly) time-dependent dynamical variables of the TCTMB molecules. $i\Omega_A$ is a resonance operator, which is null when the coupling between even and odd variables is zero, as in our treatment, which is restricted to autocorrelations. ϕ_A is the usual memory matrix and $F_A(t)$ the random force vector. In this note we need to extract from eqn (1) a *continuous* loss profile covering about nine decades of frequency, peaking at kHz and THz frequencies. This may be achieved by casting the matrices of eqn (1) in the form used by Coffey *et al.*[9] for dielectric response functions and Damle *et al.*[10] for neutron scattering:

$$A(t) = \begin{bmatrix} \dot{\theta}(t) \\ \dot{\psi}(t) \end{bmatrix}; \qquad \phi_A(t) = \begin{bmatrix} \beta_2\delta(t)+\omega_0^2; & -\omega_0^2 \\ -\Omega_0^2 \quad ; & \beta_1\delta(t)+\Omega_0^2 \end{bmatrix};$$

$$F_A(t) = \begin{bmatrix} \dot{W}_2(t) \\ \dot{W}_1(t) \end{bmatrix}. \tag{2}$$

Here θ and ψ are angles defined previously.[9] The frequency ω_0 is effectively that of the THz peak, and

$$\Omega_0 = (I_2/I_1)\,\omega_0$$

where the moments of inertia I_2 and I_1 refer to the molecule and the nearest neighbour cage respectively. W_2 and W_1 are Wiener processes representing the stochastic part of the total torque and β_1 and β_2 are friction coefficients respectively between the outer cage and its surroundings and between the inner molecule and its nearest neighbour cage. We stress that the mathematics apply to the angular variation of dipoles embedded in asymmetric tops, provided that the reorientation is confined to a plane, as in the TCTMB hexad librations. It is natural in TCTMB to expect that $\beta_1 \gg \beta_2$ since the collective reorientation is analogous to the α and β processes observed by Johari *et al.*[11] in viscous liquids and glasses and is very slow compared with the libration of individual molecules.

Recently Coffey has shown[7] that the set of matrices (2) defines also an electrodynamic process of dipole–dipole interaction superimposed on rotational diffusion as first discussed by Budo. For details, the reader is referred to the paper by Coffey. Briefly, a measuring field is applied in the same plane of rotation of a pair of dipoles $\boldsymbol{\mu}_1$ and $\boldsymbol{\mu}_2$ which rotate about an axis through their common centre perpendicular to the plane containing the field. A harmonic dipole–dipole coupling potential with frequency ω_0 is chosen and I_1 and I_2 are defined as the moments of inertia of the dipoles $\boldsymbol{\mu}_1$ and $\boldsymbol{\mu}_2$, respectively about an axis perpendicular to their own plane. β_1 and β_2 are opposing friction coefficients arising from the surroundings.

Therefore the same set of matrices (2) may be used to describe a THz resonance arising either from a purely kinematic mechanism (the itinerant librator), or a purely electrostatic, dipole–dipole, interaction superimposed upon a rotational diffusion corrected for inertial effects or, indeed, a mixture of both. The set of matrices (2) is therefore by no means an unrealistic representation of the molecular dynamics in TCTMB.

DISCUSSION

All our parameters except β_2 are defined by the available experimental data. β_1 is measured from the critical frequency of the slow diffusion process in the kHz ($\beta_1 = kT\tau_D/I_1$, where τ_D is the inverse of this peak frequency). ω_0 is the far infrared peak frequency, *i.e.*, that of the molecular libration. The cage moment of inertia I_1 can be calculated using X-ray data. The limiting case $\beta_2 = 0$ produces a very sharp

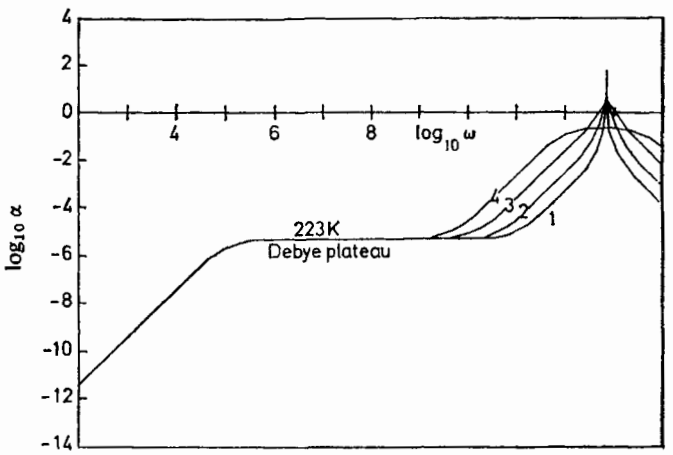

FIG. 1.—Theoretical set of curves with a series of β_2 values for TCTMB at 233 K where (1) $\beta_2 = 0.1$, (2) $\beta_2 = 0.6$, (3) $\beta_2 = 5$, (4) $\beta_2 = 50$, respectively.

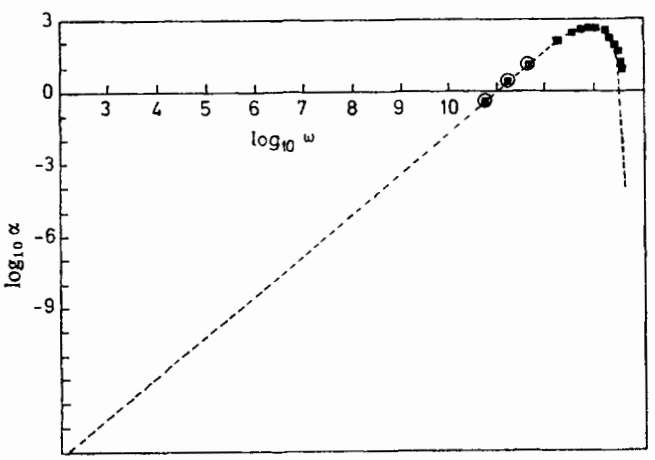

FIG. 2.—Experimental $\log_{10}\alpha(\omega)$ against $\log_{10}\omega$ plot for liquid CH_3F at 270 K. ⊛, Microwave measurements; ■, far infrared data.

resonance at far infrared frequencies but, when finite, broadens the THz profile in accord with observation. This process is shown on a log scale in fig. 1. The THz absorption is broadened considerably by increasing the friction between molecule and cage. However, the low frequency profile is left unaltered. This observation is significant because it allows us to estimate β_2 by a least mean squares fitting to

far infrared data alone. It is necessary only to know the critical frequency of the slow diffusion process to fix the low frequency absorption profile.

The $\log_{10}\alpha$ against $\log_{10}\omega$ representation of fig. 1 and 2 demonstrates the difference between eqn (2) in the disordered solid limit and in a strongly dipolar liquid, CH_3F, at 270 K. These plots emphasise the point that the experimental loss and far infrared $\alpha(\omega)$ curves are frequency domain manifestations of the same overall autocorrelation function $\langle\cos\theta(t)\cos\theta(0)\rangle$. The zero to THz profile is a *continuous* function of frequency, and of time. For TCTMB at 300 K far infrared data are available for comparison with the calculated curves of our model, and a value of $\beta_2 = 0.9$ THz provides a least mean squares best fit with experiment, with $\beta_1 = 2.77 \times 10^3$ THz and $\omega_0 = 6.124$ THz (fig. 3).

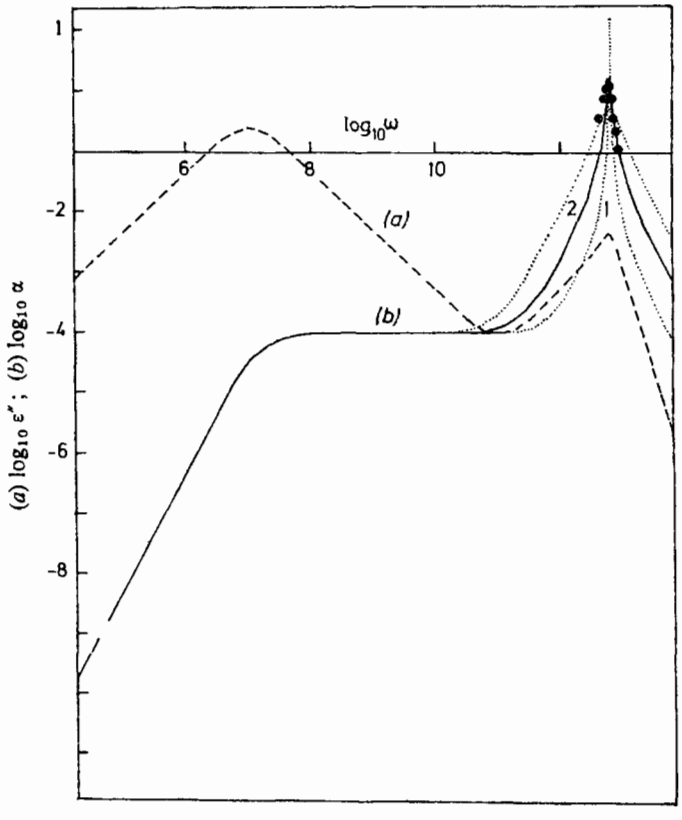

FIG. 3.—TCTMB at 300 K. —, Theoretical profile [$\alpha(\omega)$ representation]. Optimised fit is $\beta_2 = 0.9$. – –, Theoretical profile, loss representation. ●, Far infrared experimental data. . . ., (1) $\beta_2 = 0.1$; (2) $\beta_2 = 5$.

The matrices (2) are useful because the two dimensional equivalents of all the $P_n(\cos\theta)$ functions can be evaluated therefrom. It is thereby possible to calculate Rayleigh and incoherent neutron spectra by fitting the model to far infrared low frequency dielectric data. The former is proportional to the Fourier transform of $P_2[\cos\theta(t)]$ and is approximated by an $\varepsilon''(\omega)/\omega$ plot. Let us consider the distinguishing features of a depolarised Rayleigh scattering spectrum. One characteristically observes a lorentzian spectrum for small spectral shifts which yields information

concerning the reorientational motions of molecules over a long period of time. At high frequencies "shoulders" are observed (fig. 4) which yield information concerning the individual stages of the diffusive process and are a consequence of an incomplete loss of memory after collisions, *i.e.*, of non-Markovian statistics. This is directly analogous to what we observe in dielectric and far infrared experiments respectively.

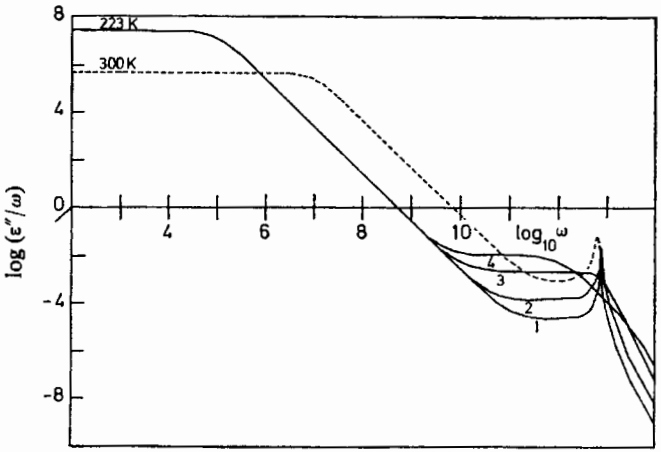

FIG. 4.—Depolarised Rayleigh scattering spectra for TCTMB at 223 and 300 K. – – –, L.m.s. best fit value of β_2 to far infrared data at 300 K. —, Theoretical set of curves at 223 K for: (1) $\beta_2 = 0.1$; (2) $\beta_2 = 2.0$; (3) $\beta_2 = 10$; (4) $\beta_2 = 50$.

The rotational part of the neutron scattering time of flight spectrum depends on all the $P_n(\cos\theta)$ functions. We intend to evaluate analytical expressions for the Fourier transforms of the general $P_n(\cos\theta)$ to first order in the polarisability [*i.e.* in the limit $kT/(I_2\omega_0^2) < 0.1$]. Therefrom, knowing $P_1(\cos\theta)$ (from far infrared/microwave results) neutron time-of-flight spectra may be also predicted.

We thank the S.R.C. for a fellowship to G. J. E. and an equipment grant. M. W. E. thanks the Ramsay Memorial Fellowship for the 1976-1978 Fellowship.

[1] A. Aiharo, C. Kitazawa and A. Nohara, *Bull. Chem. Soc. Japan*, 1970, **43**, 3750.
[2] I. Darmon and C. Brot, *Mol. Cryst.*, 1967, **2**, 301.
[3] I. Tanaka, F. Iwasaki and A. Aihara, *Acta Cryst, B*, 1974, **30**, 1546.
[4] See, for example, M. Davies, *Ann. Rep. Chem. Soc.*, 1970, **67**, 65; M. Evans, *Adv. Mol. Rel. Int. Proc.*, 1977, **10**, 203 (rev.).
[5] W. T. Coffey, T. Ambrose and J. H. Calderwood, *J. Phys. D*, 1976, **9**, L115.
[6] A. R. Davies and M. W. Evans, *Mol. Phys.*, 1978, **35**, 857; M. W. Evans, *Chem. Phys. Letters*, 1977, **48**, 385.
[7] W. T. Coffey, *Mol. Phys.*, 1978, in press.
[8] H. Mori, *Prog. Theor. Phys.*, 1965, **33**, 423.
[9] J. H. Calderwood and W. T. Coffey, *Proc. Roy. Soc. A*, 1977, **356**, 269; W. T. Coffey, *J. Phys. D*, 1977, **10**, L83; W. T. Coffey, G. J. Evans, M. W. Evans and G. H. Wegdam, *J.C.S. Faraday II*, 1978, **74**, 310.
[10] P. S. Damle, A. Sjölander and K. S. Singwi, *Phys. Rev.*, 1968, **165**, 277.
[11] G. P. Johari and C. P. Smyth, *J. Chem. Phys.*, 1972, **56**, 4411; G. P. Johari and M. Goldstein, *J. Chem. Phys.*, 1970, **53**, 2372; 1973, **58**, 1766.

(PAPER 8/547)